Desalination and Water Treatment
www.deswater.com
15 (2010) 149–159
March
1944-3994 / 1944-3986 © 2010 Desalination Publications. All rights reserved.
doi: 10.5004/dwt.2010.1679

Large-pore membrane filtration with coagulation as an MF/UF pretreatment process

Yongjun Choi[a], Hyunje Oh[b,c], Sangho Lee[b], Yunjeong Choi[b], Tae-Mun Hwang[b*,c], Gyu-Seok Baek[c], Youn-Kyoo Choung[c]

[a]*University of Science and Technology, 113 Gwahangno, Uuseong-Gu, Daejeon 305-333, Korea*
[b]*Korea Institute of Construction Technology, 2311 Daehwa-Dong, Ilsan-Gu, Goyang-Si, Gyeonggi-Do 411-712, Korea*
[c]*Department of Civil and Environmental Engineering, Yonsei University, Sinchondong 134, Sudaemungu, Seoul 120-749, Korea*
Tel. +82 (31) 910-0741; Fax +82 (31) 910-0291; email: taemun@kict.re.kr

Received 12 November 2009; Accepted in revised form 24 December 2009

ABSTRACT

MF/UF provides an effective means for removing particles and microorganisms from a feed stream via a sieving mechanism. A major obstacle to further incorporation of the membrane processes in water treatment plants, however, is the transmembrane pressure increase caused by the contaminants or pollutants in the surface water in spite of the use of coagulation and sedimentation as pretreatment processes. Therefore, a more effective process, such as prefiltration, should be considered for the pretreatment of drinking water to enhance the membrane process. In this study, a large-pore membrane filtration system with coagulation was used and evaluated as a pretreatment process for drinking water treatment. The pore diameter of the large-pore membrane reaches 2.0 μm, thus allowing for high-flux filtration under low pressure, and removing the particles effectively. According to the results of the present study, the large-pore membrane filtration system with coagulation can be used as an effective pretreatment process for drinking water because of its high turbidity and algae removal efficiency. Three different fouling models were used in this study to analyze the filtration characteristics: the pore constriction, pore breakage, and cake formation models. The major fouling mechanisms were determined to be cake formation in winter and pore breakage in spring.

Keywords: Large-pore membrane; Pretreatment; Model

1. Introduction

Recent times have seen a gradual increase in a number of applications of treatment processes using membrane filtration, thanks to the technology development and slashed economic costs in such new filtration treatment technology [1]. Compared to the conventional process, the membrane filtration process has lesser space constraints. Moreover, its automation allows easy operation, along with fewer staff requirements. It also requires small amounts of such chemicals as coagulants, thus leading to a decrease in the use of chemicals and in the generation of sludge, and subsequently, to the reduced cost of processing sludge [2]. In general, MF or UF are dominant players in the drinking water treatment process as they have relatively large pores and can be operated under a low operating pressure [2]. Such membranes are known to be effective in removing anti-chlorine pathogenic microbes, such as *Cryptosporidium* and *Giardia*, and viruses [3]. Difficulties remain, however, in the selection of effec-

* Corresponding author.

Presented at SeaHERO Academic Workshop on Development and Optimization of SWRO Desalination Systems
Korea University, Seoul, Korea, November 13–14, 2009

tive membranes and operating methods according to the characteristics of raw water. There are also some problems in the use of membranes in terms of management, such as an increase in the operating pressure triggered by membrane fouling, the washing method used, the washing intervals, the replacement interval, and the replacement costs [4]. In particular, the sole operation of membranes triggers the escalation of the operating pressure, which results from an increase in membrane fouling, thus leading to the need for an effective pretreatment processing. For such pretreatment process, coagulation and sedimentation are most commonly used. In South Korea, however, the main source of drinking water is the river, and the characteristics of seasonal weather conditions have a great impact on the changes in water temperature, the most critical factor affecting the performance of the membrane filtration process. Moreover, the torrential downpours in summer cause high turbidity, while in spring or fall, an outbreak of algae, which is a typical hampering substance in the filtration process, occurs, thus leading to repeated changes in the quality of the feed water. Such issues are attributable to the sharp increase in pollutant loading in the membrane filtration process causing poor operation of the coagulation sedimentation process, thus leading to a decrease in the production efficiency of drinking water.

The use of a large-pore membrane is a kind of microfiltration process developed to remove anti chlorine pathogenic microbes such as *Cryptosporidium* and *Giardia* [5]. The pore diameter of a large-pore membrane was set at 1–2.5 μm, enabling an excellent removal of pathogenic microbes and particles [5]. Moreover, it can operate under lower pressure with a much higher filtration flux compared to the MF/UF process leading to the possibility of its utilization in the MF/UF pretreatment process. The results of the test on the filtration characteristics of backwashing wastewater in the membrane filtration process and treatment methods show that in the membrane filtration test with 50 NTU raw water and a 100 NTU high turbidity concentration, the transmembrane pressure remained steady within 60–100 L/m^2-h filtration flux range, along with a very low remaining membrane permeate turbidity, within the range of 0.3–0.5 NTU. It also appeared that the transmembrance pressure under the high-flux operating condition of 100 L/m^2-h remained steady at an average of 5 kPa showing a very high permeability level. Accordingly, the objective of this study was to apply coagulation/large-pore membrane filtration as a pretreatment process that reduces the MF/UF process loadings according to the changes in the drinking water quality, followed by an analysis of the filtration efficiency and the membrane fouling mechanisms as well as a review of its applicability as the pretreatment process of the large-pore membrane MF/UF filtration treatment process. For the analysis of the efficiency of the large-pore membrane filtration process, a water quality comparison was made using the coagulation/sedimentation process of the existing pretreatment process. For the analysis of the membrane-fouling mechanisms, the existing membrane fouling models based on the concept of critical flux were applied.

2. Theory

Three membrane fouling models have been used to explain the transmembrane pressure increase associated with particle deposition during membrane filtration: the pore blockage, pore constriction, and cake formation models [6,7]. The following two assumptions were used for the model derivation. First, it was assumed that particle deposition occurs only when the operating permeate flux $J(t)$ exceeds the critical flux (J_c). Second only one fouling models is predominant in each case. This assumption is justified because we aim at determining the major fouling mechanism. The fouling models may be applied using either of two methods. First, the model can be used to find the system parameters including critical flux and the model constant by fitting the model with experimental data. Second, from the model parameters and model equation obtained via fitting, the variation profile of the transmembrane pressure can be predicted under various operating conditions. The performances of the fouling models were evaluated based on the comparison of the predicted and experimental transmembrane pressure. The prediction of the fouling models was done based on the most widely used criteria, the root mean square error (RMSE).

2.1. Pore blockage model

Pore blockage, which contributes significantly to membrane fouling during the blockage of the membrane pores, occurs when the particles are approximately the same size as the membrane pores. When pore blockage is present, the transmembrane pressure increases rapidly. The separation properties are mainly determined by the membrane. The operating flux can be calculated as a function of total filtration resistance $R_t(t)$ using Darcy's law

$$J = \frac{\Delta P(t)}{\mu R_t(t)} \tag{1}$$

where $\Delta P(t)$ is the transmembrane pressure and μ is the solution viscosity. In the pore blockage model, the rate of changes in the membrane area blocked by particles is assumed to be directly related to the rate of particle convection to the membrane surface. Thus the membrane area blocked by particles is:

$$A_b = \alpha(J - J_c)C_b t \tag{2}$$

where A_b is the membrane area blocked by particles, α is the complete blockage model constant, J is the operating flux, J_c is the critical flux, C_b is the concentration of deposits in bulk phase and t is the operating time. Thus, the ratio of the membrane area blocked by particles is:

$$\frac{R_t(t)}{R_t(0)} = \left(1 - \frac{A_b}{A_m}\right)^{-1} = \left(1 - \frac{\alpha(J - J_c)C_b t}{A_m}\right)^{-1} \quad (3)$$

where A_m is the initial membrane area. Rearranging Eq. (3), $R_t(t)$ is:

$$R_t(t) = R_m \left(1 - \frac{\alpha(J - J_c)C_b t}{A_m}\right)^{-1} \quad (4)$$

where $R_m = R_t(0)$ is the intrinsic membrane resistance. Substitution of Eq. (4) into Eq. (1) yields

$$J = \frac{\Delta P(t)}{\mu R_m}\left(1 - \frac{\alpha(J - J_c)C_b t}{A_m}\right) \quad (5)$$

And then rearranging Eq. (5), $\Delta P(t)$ is:

$$\Delta P(t) = P_0 \left(1 - \frac{\alpha(J - J_c)C_b t}{A_m}\right)^{-1} \quad (6)$$

where $P_0 = \mu R_m J$ is the initial transmembrane pressure.

2.2. Pore constriction model

Pore constriction is possible only for membranes with relatively large pores, which are easily accessible to the particles. Fouling consists of pore constriction involving the adsorption of particles onto the surface of the membrane. The extent of this mode of membrane fouling is highly dependent on the morphology of the membrane. In the pore constriction model, a change in deposited mass over time can be derived from the mass balance as:

$$-\frac{1}{\rho_d}\frac{dm_d}{dt} = N(2\pi r_p)\delta\frac{dr_p}{dt} \quad (7)$$

where m_d is the deposited mass of foulants, N is the number of pores on the membrane, δ is the pore length, r_p is the pore radius and r_d is the density of the deposits. By integrating Eq. (7), the reduction of pore is:

$$\frac{r_p(t)}{r_{p,0}} = \left(1 - \frac{m_d}{\pi N \delta \rho_d}\right)^{1/2} = (1 - \beta m_d)^{1/2} = (1 - \beta(J - J_c)C_b t)^{1/2} \quad (8)$$

where β is the pore constriction model constant, $r_{p,0}$ is the pore radius before fouling and m_d is assumed to be directly related to the rate of particle convection to the membrane surface.

Using the Hagen–Poiseuille equation and Darcy's law, the permeate flux is:

$$J = \frac{1}{A_m}\frac{\pi r_{p0}^4 N}{8\mu\delta}(\Delta P(0)) = \frac{\Delta P(0)}{\mu R_t(0)} \quad (9)$$

where $\Delta P(0)$ is the initial transmembrane pressure and $R_t(0)$ is the initial filtration resistance. Thus, the initial filtration resistance $R_t(0)$ is proportional to r_{p0}^{-4}. Thus, the ratio of the filtation resistance is:

$$\frac{R_t(t)}{R_t(0)} = \left(\frac{r_p(t)}{r_{p,0}}\right)^{-4} \quad (10)$$

Substitution of Eq. (8) into Eq. (10) yields

$$R_t(x,t) = R_m\left(1 - \beta(J - J_c)C_b t\right)^{-2} \quad (11)$$

Substitution of Eq. (11) into Eq. (1) yields

$$J = \frac{\Delta P(t)}{\mu R_m}\left(1 - \beta(J - J_c)C_b t\right)^2 \quad (12)$$

And then rearranging Eq. (12), $\Delta P(t)$ is

$$\Delta P(t) = P_0\left(1 - \beta(J - J_c)C_b t\right)^{-2} \quad (13)$$

2.3. Cake formation model

Cake formation appears to have a significant effect on the increase in transmembrane pressure during the formation of cake layers on the membrane surface. This effect tends to occur when the particle forms aggregates. The aggregates are essentially particles that have flocculated and that have been deposited on the surface of the membrane, forming a cake layer. In the cake formation model the total filtration resistance increased by the presence of a cake layer on the membrane surface. The total filtration resistance, $R_t(t)$ will be the sum of the intrinsic membrane resistance (R_m) and the cake resistance ($R_c(t)$). Thus, the total filtration resistance is:

$$R_t(t) = R_m + R_c(t) \quad (14)$$

Substitution of Eq. (14) into Eq. (1) and then rearranging Eq. (1), $\Delta P(t)$ is

$$\Delta P(t) = \mu R_m J + \mu R_c(t) J = P_0 + \mu R_c(t) J \quad (15)$$

Based on the concept of critical flux, Eq. (15) can be rewritten as follows:

$$\Delta P(t) = P_0 + \mu R_c(t)(J - J_c) \quad (16)$$

Cake resistance, R_c is assumed to be directly related to the rate of particle convection to the membrane surface.

$$R_c(t) = \gamma(J - J_c)C_b t \quad (17)$$

where γ is the cake formation model constant. Substitution of Eq. (17) into Eq. (16) yields

$$\Delta P(t) = P_0 + \gamma(J - J_c)^2 \mu C_b t \quad (18)$$

3. Materials and methods

In this study, membrane feed water was sampled, which was subjected to the mechanical mixing/coagulation process in an MF membrane filtration pilot plant with a capacity of 50 m^3/d using the Han River water as raw

water. The coagulant chemical in the pilot plant uses 17% PACl, and its injection amount was determined according to the jar test with the injection range of 5–10 ppm. The large-pore membrane filtration test was conducted at the lab scale. Fig. 1 shows an outline of the test equipment that was used.

In this study, large-pore microfiltration membrane hollow-fiber modules were adopted. Table 1 shows the membrane characteristics. The membrane filtration test equipment was operated through the dead-end filtration method with constant flow control. Following 10 min filtration, 30 s air backwashing was carried out under 30 kPa pressure in the reverse direction of filtration. The filtration membrane pore size was set at 2 μm with the vertical-membrane module. Its length was 27 cm, and the membrane area was set at 0.05 m^2.

As for the sedimentation test, the water after the coagulation process of the pilot plant process was sampled, followed by 120-min long sedimentation in a 3 L container. The supernatant from the container was then analyzed. The large-pore membrane test equipment was operated under various fluxes (105–170 L/m^2-h) for the analysis of the filtration characteristics. For the analysis of the characteristics of raw-water quality and settling water, and of the large-pore membrane microfiltration filter water, the following were measured: temperature (°C), turbidity (NTU), UV_{254} (abs/cm–1), TOC (mg/L), DOC (mg/L), and chlorophyll-a (mg/m^3).

Table 1
MF membrane specifications

Items	Values
Filtration method	Dead end
Flow type	Outside-in
Membrane type	Hollow fiber
Material	Polysulfone
Pore size, μm	2.0
Module length, cm	27
Membrane area, m^2	0.05

4. Results and discussion

4.1. Characteristics of raw water quality

Fig. 2 shows the seasonal characteristics of raw water in the Han River, which demonstrates a large change in turbidity, chlorophyll-a, TOC, and temperature according to the season. The TOC appeared to be high in winter (January–February), while chlorophyll-a appeared to be high in spring and fall, and turbidity in summer. For the raw water quality, the water temperature appeared to be a highly critical factor influencing the performance of the membrane process, which was determined to have a minimum of 1.1°C and a maximum of 28.4°C. The average temperature in summer was 23°C, while in winter, it was 3°C. The low average temperature in winter increases the water viscosity approximately by 13% compared to summer, leading to an about 11.7% decrease in the pure permeate flux.

4.2. Results of the analysis of the sedimentation treatment water/large-pore membrane filter water quality

Fig. 3 shows the results of the analysis of the sedimentation treatment water and large-pore membrane permeate in winter, at low water temperatures (average water temperature: 5.5°C). The simple comparison of the aver-

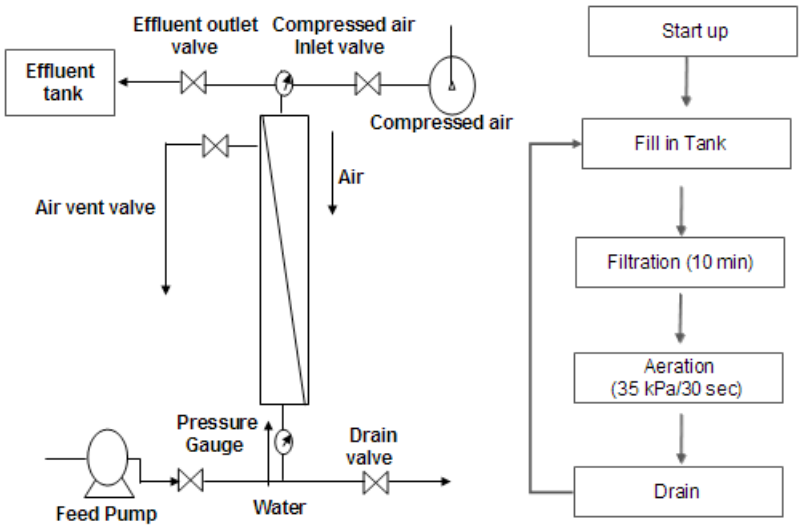

Fig. 1. Schematic diagram and control logic of the large-pore membrane system.

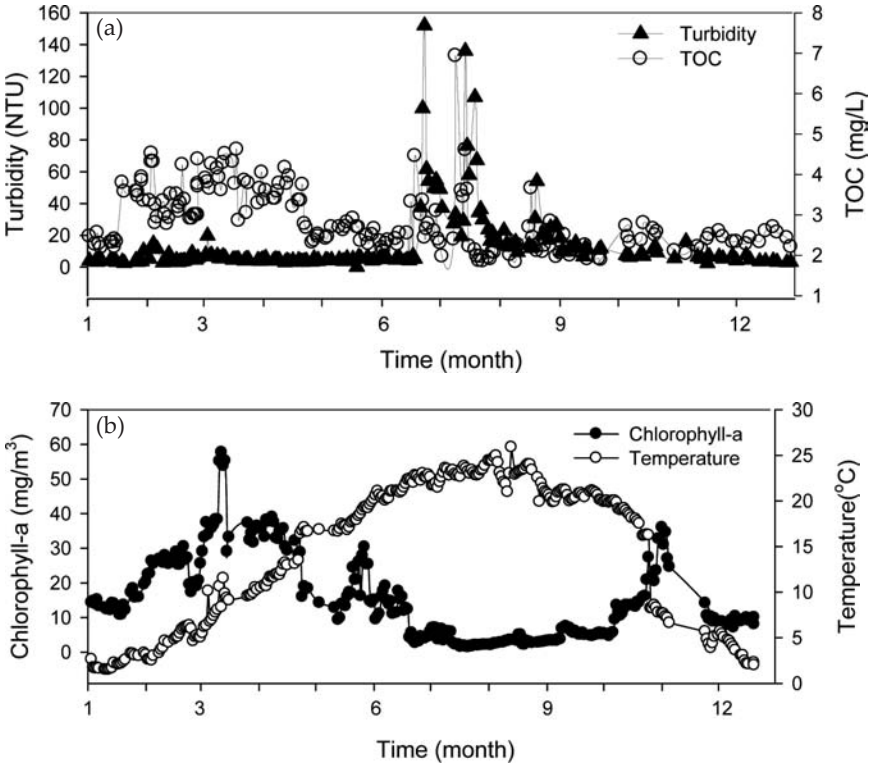

Fig. 2. Seasonal variations of raw water quality in the Han River: (a) Turbidity and TOC (b) Algae and temperature.

ages of the quality of each of the aforementioned kinds of water showed that the large-pore membrane filtration process was superior in turbidity and chlorophyll-a removal compared to the sediment treatment process, but in the removal of such substances as UV_{254}, TOC, and DOC, it showed somewhat low efficiency.

Fig. 4 shows the results of the analysis of water quality in the sedimentation process and the large-pore membrane filtration process in spring, when an algae outbreak occurs. Following the simple comparison of the averages of the water quality factor of each of the two kinds of water tested, it appeared that the large-pore membrane filtration process was superior in removal turbidity and algae compared with the sediment treatment process, as is the case in winter, but had a similar or somewhat low efficiency in removal of such substances as UV_{254}, TOC, and DOC.

4.3. Statistical water quality comparison

In this study, to compare the water quality in the coagulation/sedimentation process with that in the coagulation/large-pore membrane filtration process during the periods of winter (with low temperatures) and spring (characterized by the outbreak of high-concentration algae), the level of significance was set at 5%, and paired *t*-test was used.

Table 2 refers to the result of the paired t-test on the comparison of water quality during the periods of winter with low temperatures. It shows that there are significant differences in turbidity, UV_{254}, and TOC and DOC between the two processes (< 0.05).

In terms of turbidity, the difference between the averages of the two processes was 1.63 NTU, showing the excellence of the large-pore membrane filtration process in terms of the removal of turbidity. As for UV_{254}, TOC, and DOC, the differences between their averages were –0.0017, –0.057, and –0.110, respectively, showing the efficiency of the sedimentation process in terms of their removal, with only a slight difference from the large-pore membrane process. As for chlorophyll-a, the concentration of the large-pore membrane filtration process appeared to be lower than the detection limit in both winter and spring, showing the insignificance of the paired *t*-test result, which was thus excluded from the analysis results.

Table 3 refers to the results of the paired *t*-test on the comparison of water quality in spring when an algae outbreak occurs. As for UV_{254} and TOC, their significance probabilities were 0.140 and 0.592, respectively, with a 0.05 or above-alpha-level significance, at which the null hypothesis cannot be rejected. This implies that there is no statistical difference between the efficiency of the two processes in removal of both UV_{254} and TOC. As for turbidity and DOC, the significance probabilities were 0.000

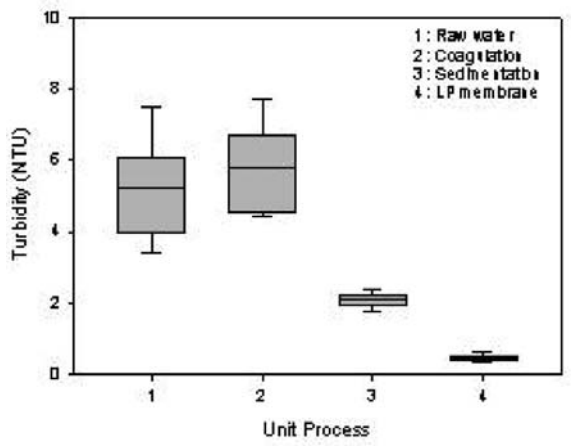

(a) Turbidity

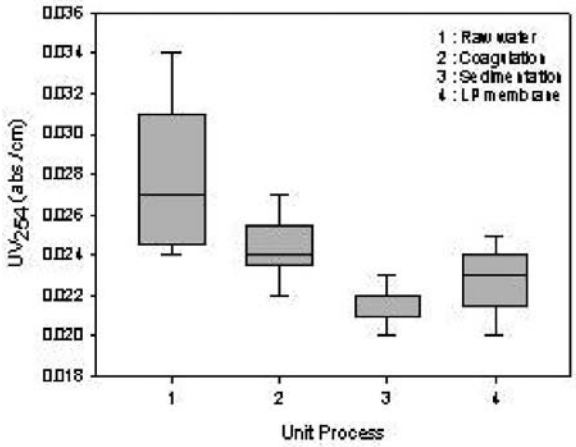

(b) UV_{254}

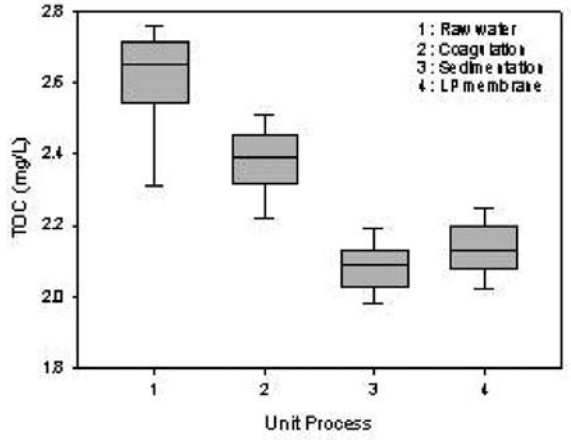

(c) TOC

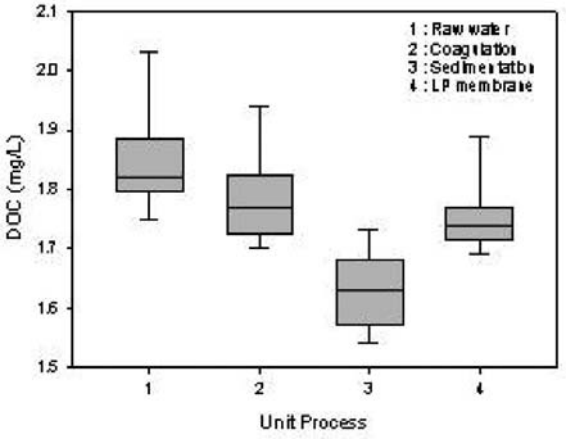

(d) DOC

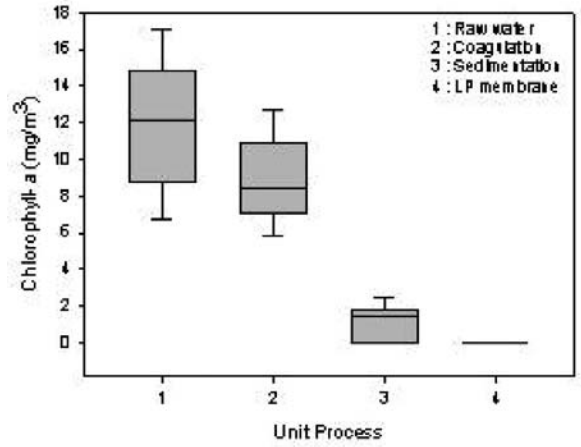

(e) Chlorophyll-a

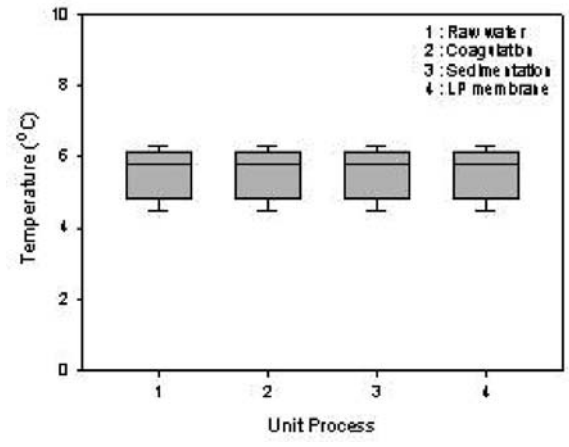

(f) Temperature

Fig. 3. Results of the analysis of water quality by unit process in winter at low water temperatures.

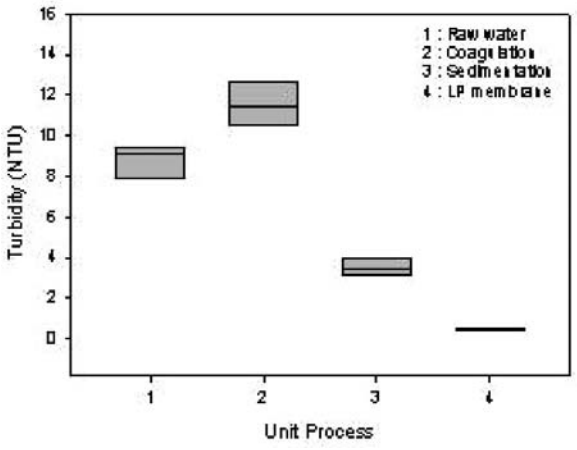

(a) Turbidity

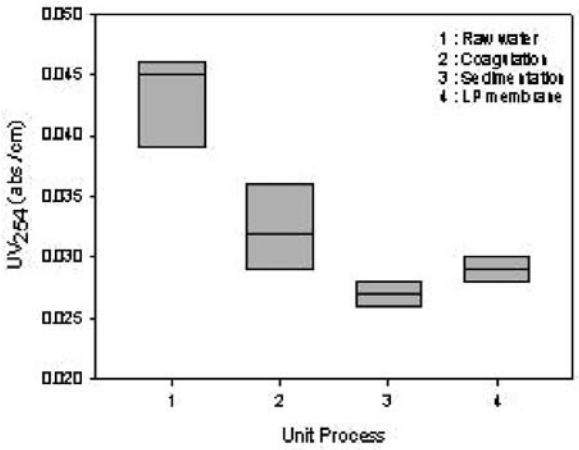

(b) UV_{254}

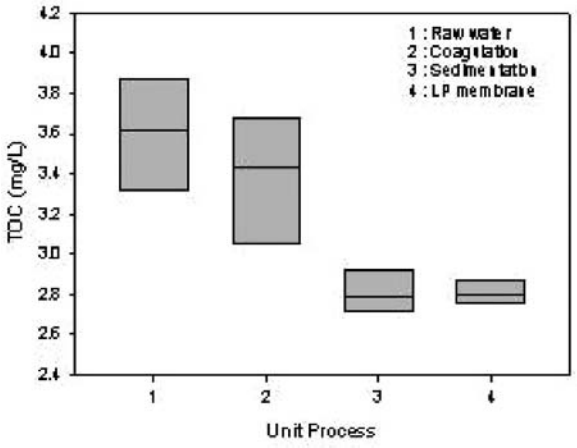

(c) TOC

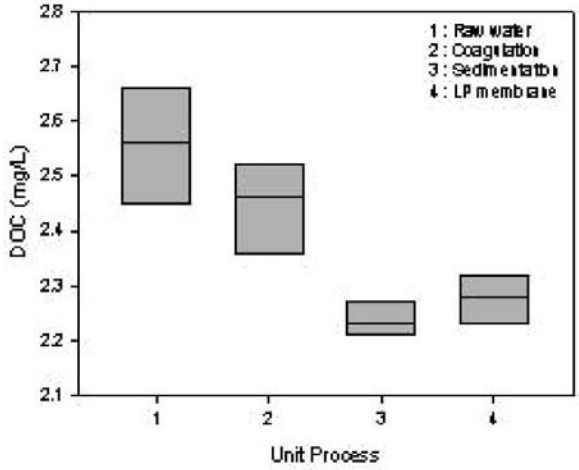

(d) DOC

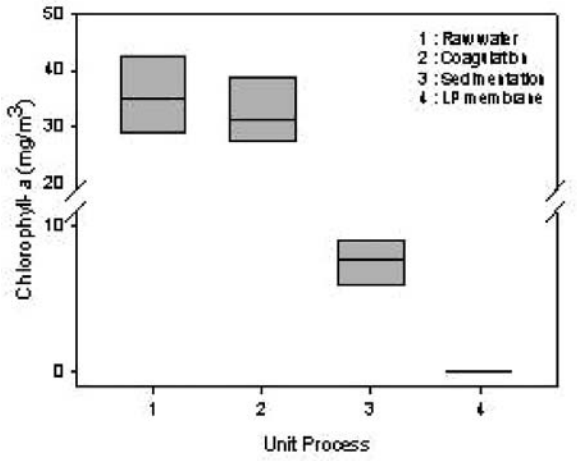

(e) Chlorophyll-a

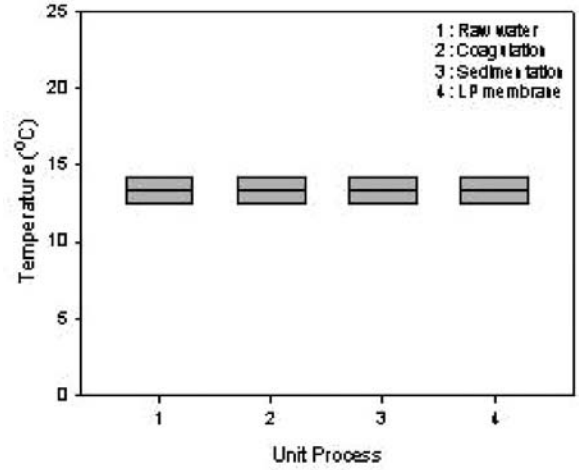

(f) Temperature

Fig. 4. Results of the analysis of water quality by unit process in spring when a high-concentration algae outbreak occurs.

Table 2
Paired *t*-test for the comparison of water quality in winter at low water temperatures

Items	Paired difference (large-pore membrane filtration water–sediment treatment water)			*t*	Degree of freedom	*p*-value
	Mean	Standard deviation	Mean difference			
Turbidity	1.63111	0.21090	0.07031	23	8	0.000
UV_{254}	–0.00177	0.00132	0.00043	–4.097	8	0.003
TOC	–0.05667	0.02062	0.00687	–8.246	8	0.000
DOC	–0.11000	0.05745	0.01915	–5.745	8	0.000

Table 3
Paired *t*-test for the comparison of water quality in spring, amidst the outbreak of algae

Items	Paired difference (large-pore membrane filtration water–sediment treatment water)			*t*	Degree of freedom	*p*-value
	Mean	Standard deviation	Mean difference			
Turbidity	3.02142	0.59327	0.22423	13.474	6	0.000
UV_{254}	–0.00071	0.00111	0.00042	–1.698	6	0.140
TOC	–0.01429	0.06680	0.02525	–0.566	6	0.592
DOC	–0.04286	0.05648	0.02135	–2.007	6	0.091

and 0.091, respectively, with a 0.05 or above-alpha-level significance, which indicates that there is a difference between the two processes in terms of water quality. As for turbidity, the difference between the averages of the two processes was 3.02 NTU, showing the excellence of the large-pore membrane filtration process in terms of the removal of turbidity, while the sediment treatment process was shown to be excellent in removal of DOC, with an average difference of –0.043 from the large-pore membrane filtration process.

4.4. Results of critical flux test

As there is a difference between the characteristics of raw water quality in the Han River in terms of turbidity, algae concentration, and water temperature in winter and spring, there is a difference as well in the characteristics of filtration between the two seasons. Accordingly, to determine the critical flux in winter and spring, the flux step method was used in this study. Fig. 5 shows the changes in the transmembrane pressure, permeability, and $\Delta P/\Delta t$ according to the increase in the flux in winter. The filtration time was set at 240 min for each step. The flux increased by 20–25 L/m^2-h at each step, beginning from 105 L/m^2-h to 170 L/m^2-h. As for the transmembrane pressure, its sensitively reacted to a change in flux. No change appeared in the transmembrane pressure under a flux of 150 L/m^2-h or below, but a sharp lineal increase under a flux of 170 L/m^2-h was shown. Moreover, the membrane permeability also appeared unstable under a flux of 170 L/m^2-h. Accordingly, it was determined that there is a critical flux in winter between 150 L/m^2-h and 170 L/m^2-h.

Fig. 6 shows the changes in the transmembrane pressure, $\Delta P/\Delta t$, and permeability according to the increase in the flux in spring. For the filtration time, 240 min was also set at each step, as in winter. The flux increased by 20–25 L/m^2-h at each step, beginning from 105 L/m^2-h to 170 L/m^2-h.

The filtration characteristics in summer appeared similar to those in winter. In terms of the transmembrane pressure, it sensitively reacted to the flux. Under a flux of 150 L/m^2-h or lower, there appeared no difference in the transmembrane pressure, but it increased exponentially under a flux of 170 L/m^2-h. Furthermore, the membrane permeability appeared unstable under a flux of 170 L/m^2-h. Accordingly, it was determined that there is a critical flux of between 150 and 170 L/m^2-h in winter.

4.5. Results of the model applications

For the analysis of the filtration characteristics of the large-pore membrane according to the season, three kinds of membrane fouling models were applied to the test results, based on the concept of critical flux: the pore constriction, pore breakage, and cake formation models. Fig. 7 shows the application of the three kinds of models to the test results of the critical flux in winter, indicating an agreement between the three models and the test results. To find the dominant membrane-fouling mechanism, the

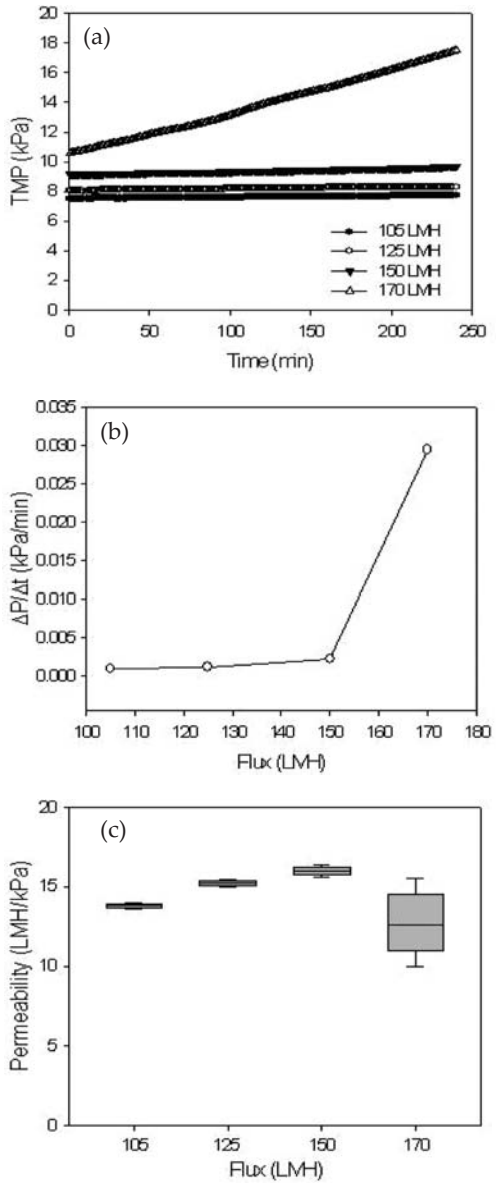

Fig. 5. Variations in (a) TMP, (b) $\Delta P/\Delta t$, and (c) permeability according to the flux in winter.

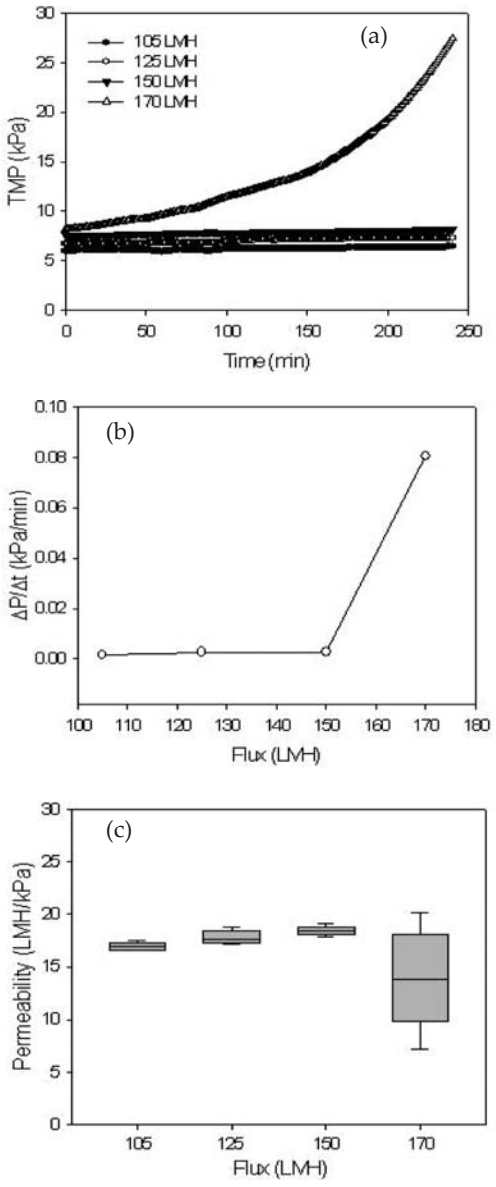

Fig. 6. Variations in (a) TMP, (b) $\Delta P/\Delta t$, and (c)permeability according to the flux in spring.

RMSE was analyzed and the model evaluation criteria were selected. As shown in Table 4, the cake formation model showed the highest level of agreement among the three models. Cake formation model constant, γ and J_c and RMSE, were determined to be 4.0×10^{12} m/kg, 160 L/m^2-h, and 0.1274, respectively.

Fig. 8 shows the application results of the pore constriction, pore breakage, and cake formation models to the test results of the critical flux in spring. Unlike in winter, the pore blockage model appeared to be the only one showing agreement among the three models. Pore breakage model constant, α and J_c and RMSE, were determined to be 73 m^4/kg, 164 L/m^2-h, and 0.2684, respectively.

5. Conclusion

In the Han River water system, the characteristics of raw water quality show big changes according to the season, prompting the conclusion that the seasons exert a great influence on the filtration characteristics of the large-pore membrane filtration process. Accordingly, it seems that the analysis of the water quality characteristics according to the season is a prerequisite to the analysis of the characteristics of large-pore membrane filtration and membrane fouling.

From the comparison of the water quality between the sedimentation process and the large-pore membrane

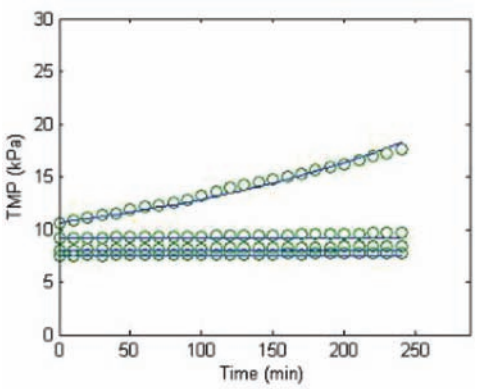

(a) Pore breakage model

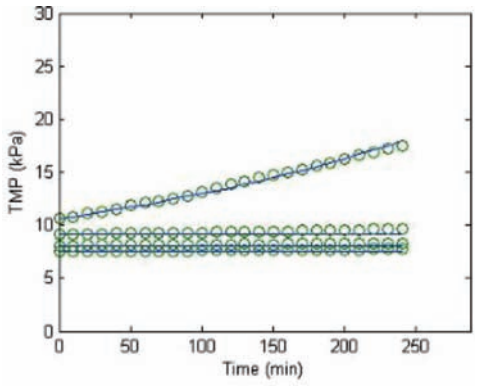

(b) Pore constriction model

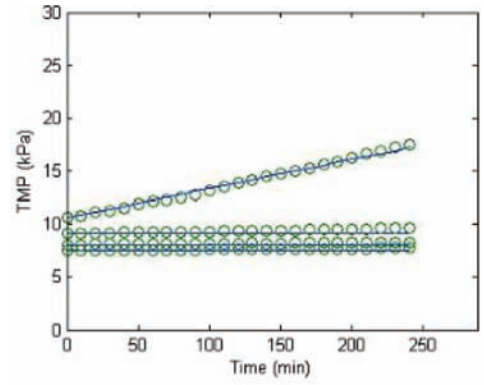

(c) Cake formation model

Fig. 7. Comparison of the models that fit the experimental data in winter.

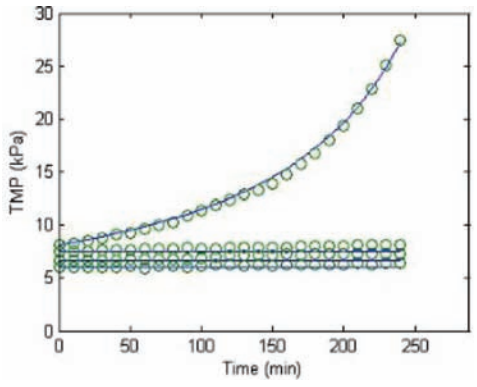

(a) Pore breakage model

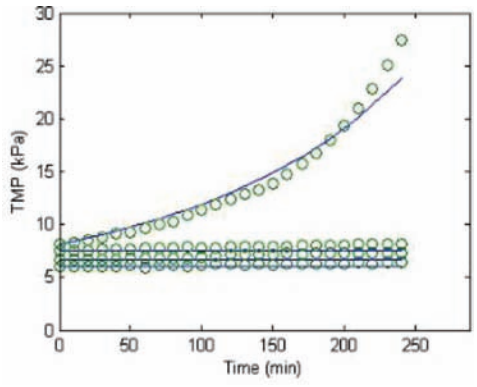

(b) Pore constriction model

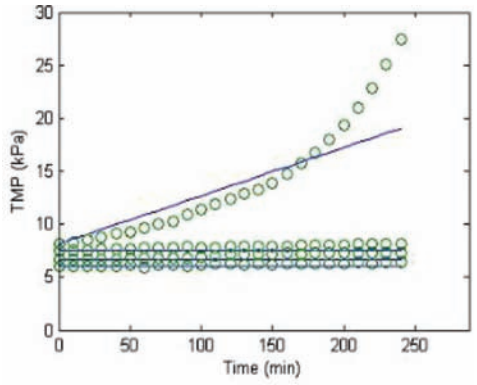

(c) Cake formation model

Fig. 8. Comparison of the models that fit the experimental data in spring.

filtration process through the paired *t*-test, it appeared that the large-pore membrane filtration process is superior in terms of the removal of turbidity and chlorophyll-a in winter, at low water temperatures compared with the sedimentation process, which showed somewhat low efficiency in removal of UV_{254}, TOC, and DOC. In spring, characterized by an algae outbreak, the large-pore membrane filtration process was shown to be superior in terms of the removal of turbidity and chlorophyll-a, as was the case in the low winter temperatures, with statistical insignificance in the elimination of UV_{254} and TOC. Its DOC removal rate appeared to be somewhat low, though. As the large-pore membrane filtration process showed a small difference from the sedimentation process in terms of the removal of TOC, DOC, and UV_{254} but showed excellence in removal of turbidity and chlorophyll-a, which are major membrane-fouling substances, in the MF/UF process, it can be said to be applicable as the pretreatment

Table 4
Comparison of the model parameters

		Winter	Spring
Pore blockage	α, m^4/kg	75	73
	J_c, L/m^2-h	163	164
	RMSE	0.2720	0.2684
Pore constriction	B, m^2/kg	580	520
	J_c, L/m^2-h	160	160
	RMSE	0.1637	0.7954
Cake formation	γ, m/kg	4×10^{12}	3.3×10^{12}
	J_c, L/m^2-h	160	160
	RMSE	0.1274	1.8237

process of the MF/UF process. A combination of appropriate post-treatment processes is needed, however, due to the impossibility of removal of the dissolved substances in the MF/UF process.

Following the application of the determined values of the large-pore membrane critical flux to the aforementioned fouling models, it appeared that the cake formation model is appropriate in winter while the pore breakage model is appropriate in spring when viewed from the aspect of the membrane fouling mechanism. The application of the three aforementioned fouling models based on the critical-flux concept seemed effective in allowing a better understanding of the membrane-fouling characteristics of the large-pore membrane.

Acknowledgements

This research was supported by a grant (07seaheroB02-01-02) from the Plant Technology Advancement Program funded by the Ministry of Land, Transport and Maritime Affairs of the Korean government.

References

[1] S.S. Adham, J.G. Jacangelo and J.-M. Lainé, Characteristics and costs of MF and UF plants, J. AWWA, 88(5) (1996) 22–31.
[2] J.G. Jacangelo, N.L. Patania, J.-M. Lainé, J.M. Montgomery, W. Booe and J. Mallevialle, Low Pressure Membrane Filtration for Particle Removal, AWWA Research Foundation, Denver, 1992.
[3] J.G. Jacangelo, S.S. Adham and J.-M. Lainé, Mechanism of Cryptosporidium, Giardia, and Ms2 virus removal by MF and UF, J. AWWA, 87(9) (1995) 107–121.
[4] B. Nicolaisen, Developments in membrane technology for water treatment, Desalination, 153 (2003) 355–360.
[5] Y. Jimbo, K. Komatsu, K. Goto aqnd T. Hirata, Development of a large pore membrane filtration system for the pathogenic protozoa removal, J. JWWA, 71(8) (2002) 11–18.
[6] A.S. Ward, Liquid Filtration Theory, Filtration, Principles and Practices, M.J. Matteson and C. Orr, eds., Marcel Dekker, New York, 1987, pp. 131–161.
[7] J. Granger, J. Dodds and D. Leclerc, Filtration of low concentrations of latex particles on membrane filters. Filtr. Separ., January/February (1985) 58–60.